HOSTED BY
ELSEVIER
CrossMark
Available online at www.sciencedirect.com
ScienceDirect
Defence Technology 11 (2015) 237–243
www.elsevier.com/locate/dt

Microstructure and pitting corrosion of shielded metal arc welded high nitrogen stainless steel

RAFFI MOHAMMED [a], G. MADHUSUDHAN REDDY [b], K. SRINIVASA RAO [a,*]

[a] *Department of Metallurgical Engineering, Andhra University, Visakhapatnam, India*
[b] *Defence Metallurgical Research Laboratory, Hyderabad, India*

Received 17 March 2015; revised 20 April 2015; accepted 21 April 2015
Available online 22 May 2015

Abstract

The present work is aimed at studying the microstructure and pitting corrosion behaviour of shielded metal arc welded high nitrogen steel made of Cromang-N electrode. Basis for selecting this electrode is to increase the solubility of nitrogen in weld metal due to high chromium and manganese content. Microscopic studies were carried out using optical microscopy (OM) and field emission scanning electron microscopy (FESEM). Energy back scattered diffraction (EBSD) method was used to determine the phase analysis, grain size and orientation image mapping. Potentio-dynamic polarization testing was carried out to study the pitting corrosion resistance in aerated 3.5% NaCl environment using a G*ill*AC electrochemical system. The investigation results showed that the selected Cr–Mn–N type electrode resulted in a maximum reduction in delta-ferrite and improvement in pitting corrosion resistance of the weld zone was attributed to the coarse austenite grains owing to the reduction in active sites of the austenite/delta ferrite interface and the decrease in galvanic interaction between austenite and delta-ferrite.

Keywords: High nitrogen austenitic stainless steels (HNSs); Shielded metal arc welding (SMAW); Cromang–N (Cr–Mn–N); Field emission scanning electron microscopy (FESEM); Energy back scattered diffraction (EBSD)

1. Introduction

Austenitic stainless steels are generally used where excellent corrosion resistance and good formability are required. The development of austenitic stainless steel with improved properties was initiated in 1960s and became widespread in the 1980s [1]. In general austenitic stainless steels contain nickel as an alloying element to stabilize the austenitic phase and provide corrosion resistance to some extent [2]. Earlier improvements were related to the increase in chromium, molybdenum and nickel contents [3]. Recently much interest has been expressed in raising the level of dissolved nitrogen in the steel. The later development of the so-called high nitrogen austenitic stainless steel (HNS) with nitrogen levels sometimes exceeding 0.5 wt% has resulted in austenitic stainless steel with an exceptional combination of strength, toughness and corrosion resistance. Nitrogen is one of the alloying elements which may be used to replace the Ni addition and has the additional benefits to increase the pitting corrosion resistance and enhance the strength levels of the steel.

In fabricating the structural non magnetic material, welding is one of the most commonly used technique for joining high nitrogen austenitic stainless steels. During welding, it is essential to avoid nitrogen losses which could result in loss of mechanical properties and corrosion resistance. In order to reduce the risk of nitrogen induced porosity, the solubility of nitrogen in the weld metal has to be high enough to accommodate any increase in nitrogen concentration. The defects like porosity and solidification cracking can be overcome by the use of suitable filler wire which produces required amount

* Corresponding author.
E-mail addresses: raffia.u@gmail.com (RAFFI MOHAMMED), gmreddy_dmrl@yahoo.com (G. MADHUSUDHAN REDDY), arunaraok@yahoo.com (K. SRINIVASA RAO).
Peer review under responsibility of China Ordnance Society.

http://dx.doi.org/10.1016/j.dt.2015.04.002

of delta ferrite in the weld metal. Due to the high nitrogen content, welding requires special care to ensure that the nitrogen remains in the metal during welding [4]. Depending on service requirement, delta-ferrite content in stainless steel welds is often specified to ensure that weld metal contains a desired minimum and/or maximum ferrite level [5]. Nitrogen diffusion into the weld metal from the base metal (adjacent to the fusion line) at the elevated temperatures encountered during the weld thermal cycle could also play a role. If the nitrogen level exceeds the limit of solubility at any time during or prior to solidification in welding, the nitrogen bubbles can form in the liquid, thereby increasing the likelihood for nitrogen induced porosity [6]. In order to reduce the risk of nitrogen-induced porosity, the solubility of nitrogen in the weld metal has to be high enough to accommodate any increase in nitrogen concentration. As chromium and manganese are known to increase the solubility limit of nitrogen in austenitic stainless steel, the high levels of these elements are desired in the weld metal when filler wires for welding are selected. Another problem existing in welding a highly alloyed austenitic stainless steel is hot cracking. As a measure to minimize the hot cracking risk, one needs to choose a filler material with low impurity levels (e.g. *S*, *P*) in addition to focus on the least degree of segregation of the major alloying elements and the minimization of the level of intermetallic phase in the weld metal [7]. Nitrogen alloying can also play an important role in retarding the precipitation of intermetallic compounds [8], raising the ferrite/austenite transformation temperature and assisting the formation of austenite phase in heat affected zone of a weldment No matching filler wire is commercially available similar to the composition of the base metal (HNS). In the present work authors made an attempt to study the shielded metal arc welds of high nitrogen austenitic stainless steel using a nearest matching electrode of Cr-Mn-N type as it is presently available. Most of the researchers discussed the pitting corrosion resistance of this type of alloy, but the studies related to the welds are scarce. In view of the above, authors made an attempt to investigate the microstructural changes on pitting corrosion behaviour of weld metals of the high nitrogen stainless steel arc welds in 3.5% NaCl solution and to compare with that of the base metal, namely high nitrogen stainless steel (HNS).

2. Materials and methods

High nitrogen austenitic stainless steel (HNS) plates in cold worked condition are used in the present study. Schematic diagram of joint geometry and plate dimensions are given in Fig. 1. A set of plates with single-V butt joint welded using shielded metal arc welding (SMAW) and an electrode of Cromang-N steel (17Cr−17Mn−0.36N) was chosen in present study, as shown in Fig. 2. The compositions of base metal and electrode are given in the Table 1. The welding parameters, such as welding current and welding speed, were optimized through many welding trials. The optimized welding parameters are given in Table 2. Metallographic examination of samples was performed. The specimen were cut into pieces,

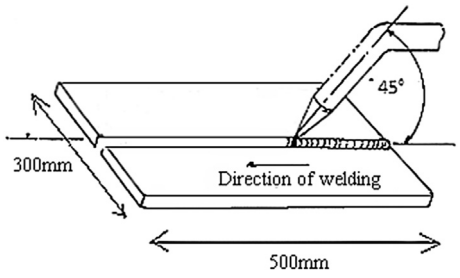

Fig. 1. Schematic diagram of joint geometry and plate dimensions.

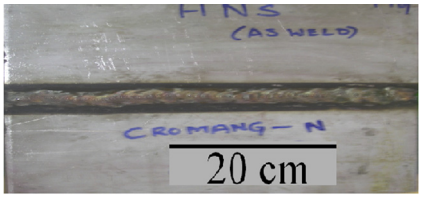

Fig. 2. Weld joint of high nitrogen steel.

which covers fusion zone, partially melted zone and heat affected zone of welds were cut, polished and etched using aqua regia reagent (HCl − 75 vol% and HNO_3 − 25 vol%). Microstructures were recorded using an optical microscope and a field emission scanning electron microscopy (FESEM) was used to examine the structural morphologies. Phases were analyse using X-Ray diffraction technique. Orientation imaging microscope (OIM) studies were done to find the orientation of the grains and the amount of different phases in the various zones of weldment using Energy back-scattered diffraction (EBSD) method. The pitting corrosion resistances of base metal and welds in an electrolyte of 3.5% NaCl were tested using a software based *GillAC* electrochemical system. The exposure area for these experiments was 0.3 mm^2.

3. Results and discussion

Addition of Chromium and Manganese increase the solubility of nitrogen whereas nickel reduces the solubility of nitrogen. Therefore the nitrogen content in Fe−Cr−Ni alloys is much lower than that in Fe−Cr−Mn alloys with comparable

Table 1
Compositions of base metal and electrode.

Material	C	Mn	Cr	N	S	P	Ni	Si	Fe
Base metal (HNS)	0.076	19.78	17.96	0.543	0.007	0.051	–	0.340	Bal.
Electrode (Cromang-N)	0.066	17.36	17.33	0.366	0.017	0.047	0.09	0.522	Bal.

Table 2
Optimized parameters for welding using shielded metal arc welding machine.

Welding current/A	Welding speed/(mm·s^{-1})	Electrode diameter/mm	Electrode position	No. of passes	Root gap/mm
110−130	4	3.2	45°	3	1.5

concentrations of Cr. Other alloying elements like Ti, V, Nb and Zr enhance the solubility of nitrogen due to their high affinity for nitrogen, which results in nitride formation. Nitride formation has also been put forward as a possible mechanism for synergy between nitrogen and molybdenum to control the localized corrosion. Nitrogen is beneficial for pitting resistance. Like molybdenum, nitrogen also shows a strong concentration gradient in the passive film. The important requirement for welding of high nitrogen steel is the solubility of nitrogen in the weld metal. It is likely that the nitrogen content of the weld metal will decrease during welding as a result of dilution with the high nitrogen base metal. The solubility of nitrogen in binary steel at 1600°c and 1 atm. nitrogen pressure is illustrated in Fig. 3.

Welded plates of high nitrogen austenitic stainless steels are shown in Fig. 2 The weldment was examined using non destructive testing to identify the surface or sub surface defects. Welds were tested visually and non-destructively using dye-penetrant testing and radiography testing. Visual examination and penetrant testing of the welds revealed no visible surface defects whereas x-ray radiographs revealed no significant defects and observed to be a sound weld as shown in Fig. 4.

Fig. 5 shows the XRD results of base metal and weldment. It can be seen from the XRD pattern that there are numerous sharp peaks that correspond to the presence of austenite. Only the single phase of austenite was identified in the base metal and the presence of austenite and delta ferrite in the welds are observed which is very beneficial to avoid the cracking tendency.

The optical microstructure of the high nitrogen stainless steel in cold worked condition is observed to have fine equiaxed grains of austenite and annealing twins as shown in Fig. 6.

The microstructure of weld metal is fully austenitic and consists of coarse columnar austenite grains growing from the fusion boundary towards the weld centerline attributed to the high amount of chromium and manganese which helps to improve the solubility of nitrogen as shown in Fig. 7(c). At the weld interface, along the fusion boundary towards the base metal transition of coarse grains to fine grains are observed as shown in Fig. 7(b) and having maximum austenite structure due to the dilution of adjacent base metal which is having nitrogen which is completely soluble in the solid solution.

The reduction of delta-ferrite in the microstructure of Cr–Mn–N weld during solidification and in the room temperature was attributed to the presence of relatively higher amount of nitrogen and completely soluble due to the higher level of manganese content. Higher manganese level of this electrode may relieve the cracking tendency of the weld metal by combining with harmful elements such as sulphur to form inclusions. No cracks were observed in the interface of the weld joints as shown in Fig. 7(b). Scanning electron micrographs to

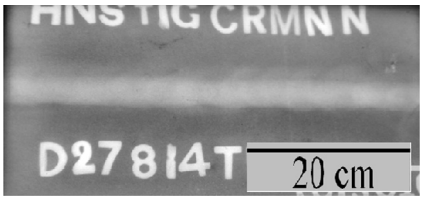

Fig. 4. X-ray radiograph of Cr–Mn–N electrode SMA weld.

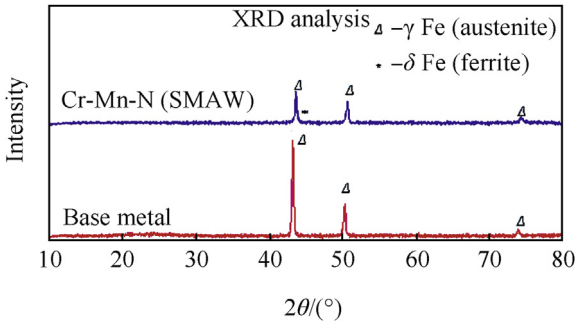

Fig. 5. XRD analysis peaks of high nitrogen steel (base metal) and SMA welds.

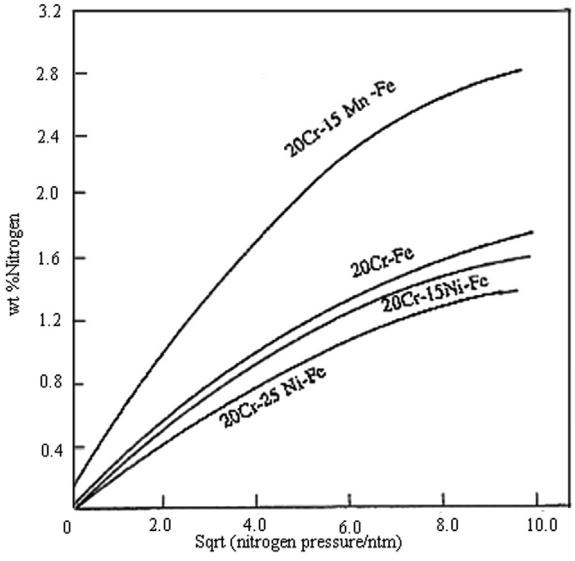

Fig. 3. Comparision of nitrogen solubilities of Ni free and Ni containing steels (Feictinger, 1988).

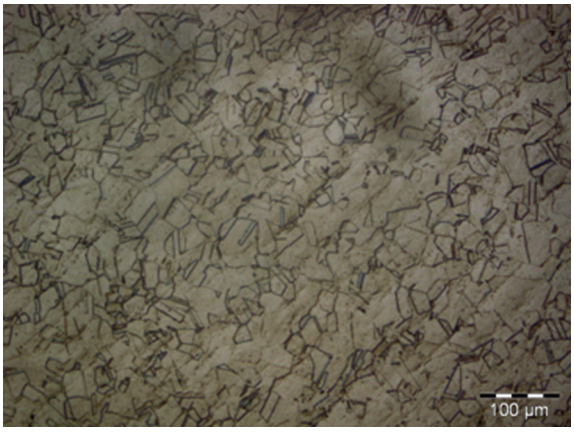

Fig. 6. Optical micrograph of high nitrogen steel (base metal).

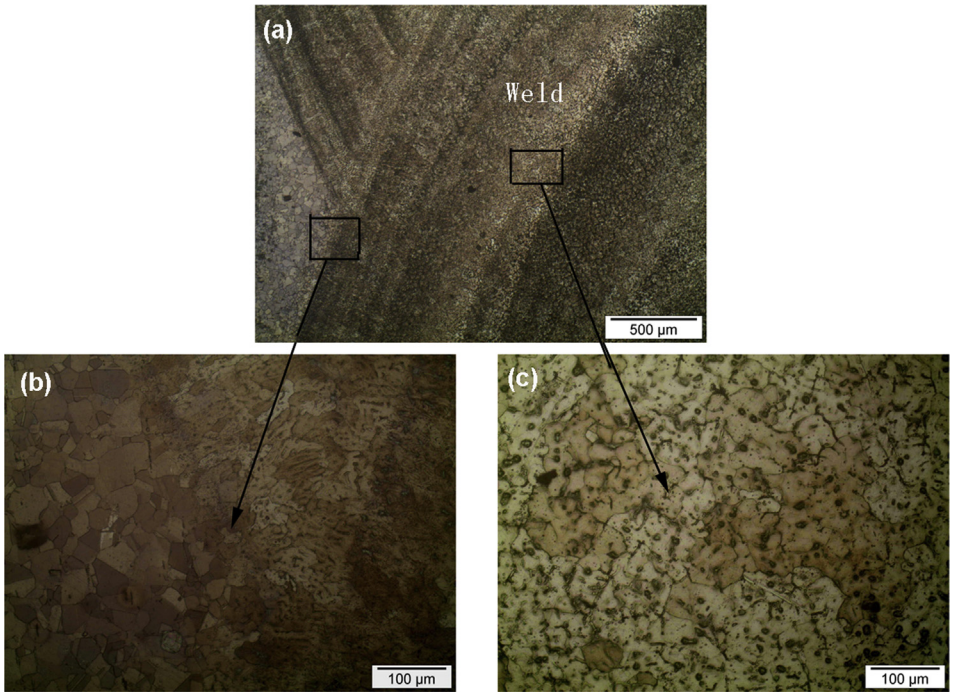

Fig. 7. Optical micrographs of high nitrogen steel welds: (a) Weld interface, (b) Heat affected zone and (c) Fusion zone.

study the microstructure at higher magnification are supportive to the optical micrograph are shown in Fig. 8.

Figs. 9–11 show the grain orientation maps and phase analysis maps of the base metal, fusion zone and weld interface of the high nitrogen stainless steel. The observations from the colour codes obtained from the orientation of grains with mis-orientation angle of 46° and OIM maps in the base metal (Fig. 9) and the orientation of coarse grains with mis-orientation angle of 28°in the fusion zone (Fig. 10)were random. The coarse grains were observed at weld interface, and the fine grains are transited from fusion zone to base metal with mis-orientation angle of 37° (Fig. 11). Different phases were analysed using phase maps, the percentage of delta ferrite and austenite were recorded, and also the distribution of

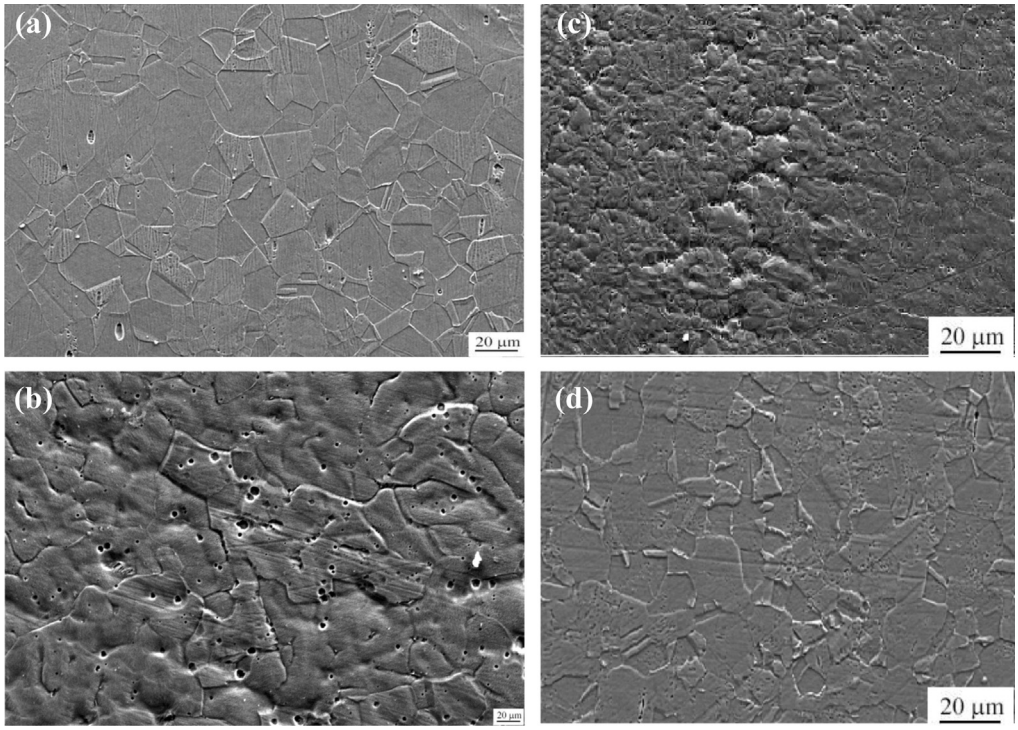

Fig. 8. SEM images of high nitrogen steel welds: (a) Base metal, (b) Fusion zone, (c) Weld interface and (d) Heat affected zone.

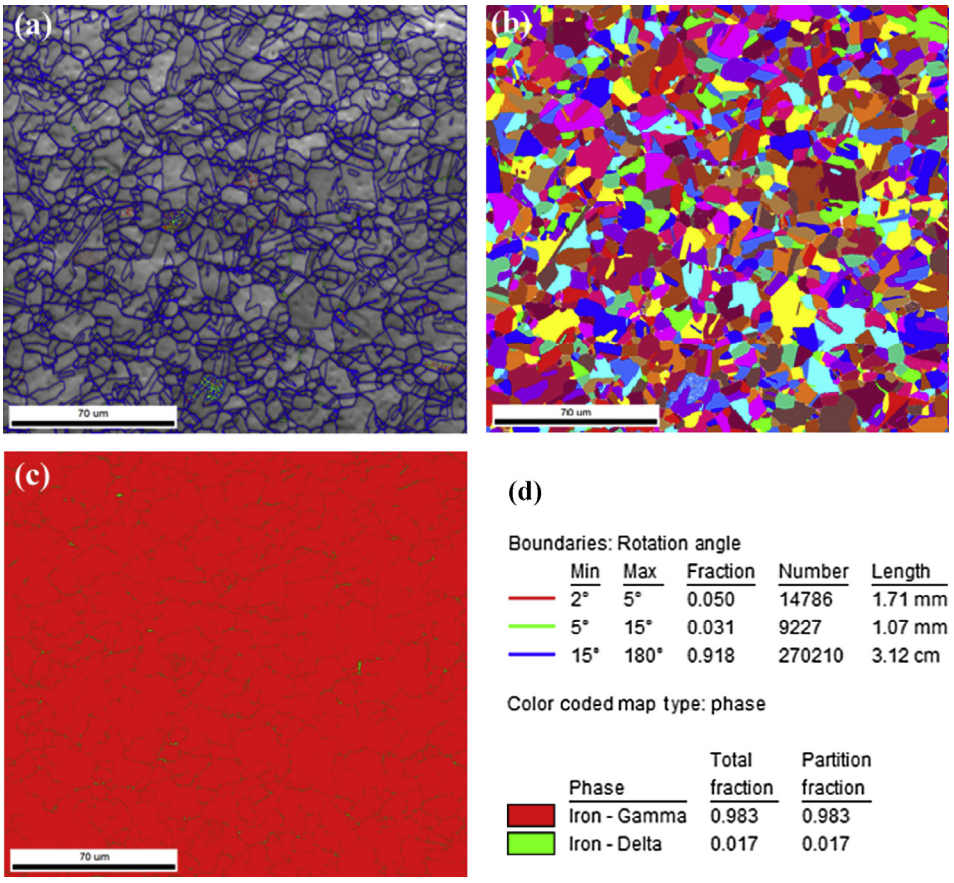

Fig. 9. Grain orientation, OIM maps and phase analysis of high nitrogen steel (base metal).

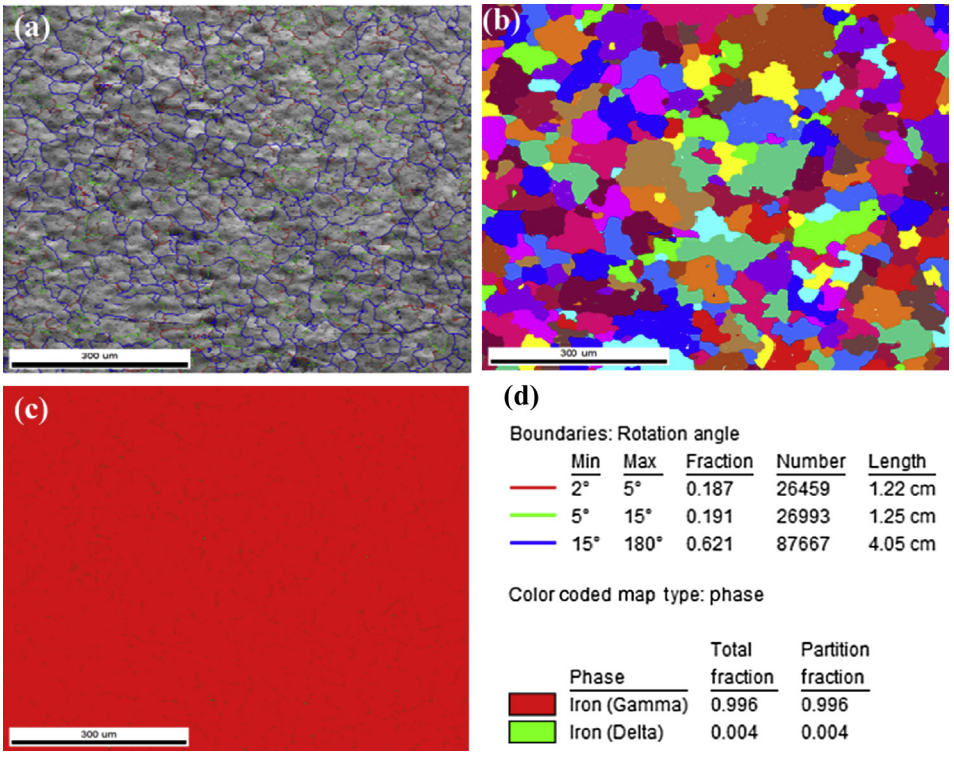

Fig. 10. Grain orientation, OIM maps and phase analysis of high nitrogen steel fusion zone.

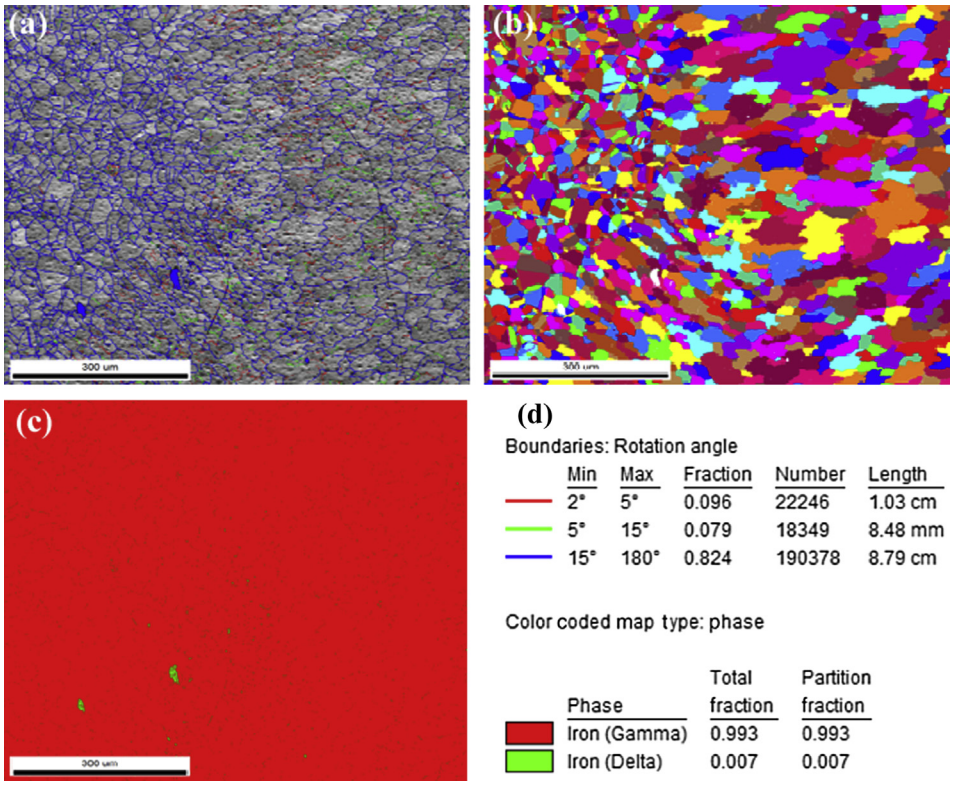

Fig. 11. Grain orientation, OIM maps and phase analysis of high nitrogen steel (weld interface).

the ferrite in the matrix was determined. It can be seen from Figs. 9–11 that the delta ferrite is distributed as discontinuous network. Percentage of ferrite, grain size, mis-orientation angle of high nitrogen steel & its welds are shown in the Table 3.

Nitrogen is a strong austenite stabilizer and its presence can lead to solid solution strengthening, resulting in an increase in strength of high nitrogen stainless steel attributed to the complete solubility of nitrogen. The high hardness values are observed compared to the weld zone in high nitrogen austenitic stainless steel as shown in the Table 4. The grain refinement and high strengthening effects in base metal of nitrogen steel could be attributed to solid solution and grain boundary strengthening mechanisms. However the formation of coarse grain in the weld zone resulted in lower hardness values.

High nitrogen stainless steel generally exhibits better localized corrosion resistance in the 3.5% NaCl solution. However, in alkaline solution, it is only varied with cold work level. The reduction in corrosion resistance was more obvious for larger prior cold worked specimens due to an enhanced precipitation process after cold working [9,10]. The cold work-dependent corrosion resistance for the High Nitrogen Stainless Steel (HNSS) in the 3.5% NaCl solution was much different from that for the N-bearing stainless steel [10]. Potentiodynamic polarization curves shown in Fig. 12 for the cold worked

Table 3
Percentage of ferrite, grain size, mis-orientation angle of high nitrogen steel & its welds.

Zone	Surface ferrite/%	Austenite /%	Average grain size/μm	Average Misorientation Angle/(°)
Base metal	1.7	98.3	3.7	46
Fusion zone	0.4	99.6	33.8	28
Interface/HAZ	3.7	99.3	15.6	37

Table 4
Vickers hardness values of different zones of weldment.

Zone	Vickers hardness(VHN)
Base metal	353
Fusion zone	279
Interface/HAZ	304

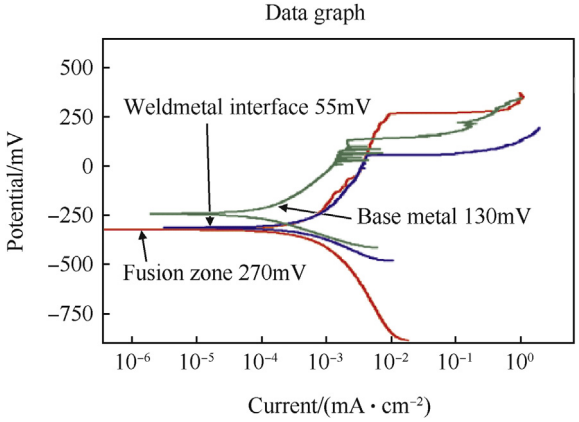

Fig. 12. Potentio-dynamic polarization of High nitrogen steel & its welds.

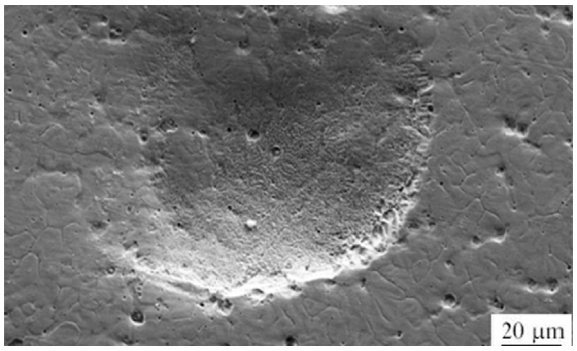

Fig. 13. Pit formation of high nitrogen stainless steel weld.

HNS base metal were analysed to study the critical pitting potential and compared with those of the HNS welds made using Cr–Mn–N electrode in 3.5% NaCl solution using a basic electrochemical cell. Repeated damages of the dislocations on the slip plane would lead to the formation of a slip band on the surface which will disturb the passive film on the surface to expose the bare material to the working environment, and chloride will start attacking and leads to the dissolution of base metal. The heterogeneities of the weld metal and the reduction of delta ferrite are beneficial to the pitting resistance and greater amounts deteriorate the pitting corrosion resistance significantly. Pit formation was observed in Fig. 13. Pitting potential values are shown in the Table 5. The composition of the alloy, grain size and corrosion potential relative to the adjacent matrix affects the corrosion behaviour. The pitting potential (Epit) of the Cr–Mn–N weld metal is observed to be more positive. The Cr–Mn–N weld metal has better corrosion resistance compared to base metal, which is attributed to the improvement in nitrogen and the reduction in delta ferrite. The lower pitting corrosion resistance of the weld metal interface is because of 3.7% delta ferrite in it. The potential difference between ferrite and austenite and the distribution of ferrite as continuous network are owing to the galvanic interaction between austenite and delta ferrite interface.

Table 5
Pitting potential values of different zones of weldment.

Zone	Pitting potential/mV
Base metal	130
Fusion zone	270
Interface/HAZ	55

4. Conclusions

1) Use of Cromang-N electrode in shielded metal arc welding of high nitrogen steel resulted in maximum solubility of nitrogen and a defect free weld was observed.
2) Microstructure of the high nitrogen steel has complete austenite grain structure with annealing twins at the boundaries as nitrogen acts as an austenitic stabilizer. The fusion zone of high nitrogen steel was observed to be solidified as austenite coarse grains and the delta ferrite was observed.
3) Grain orientation and phase analysis maps clearly shows the distribution of grains and percentage of austenite and delta ferrite in the fusion zone, weld interface and base metal
4) Improvement in pitting corrosion resistance of the fusion zone compared to base metal is attributed to the coarse austenite grains owing to the reduction in active sites of the austenite/delta ferrite interface and the decrease in galvanic interaction between austenite and delta-ferrite.

Acknowledgements

The authors would like to thank Director, Defence Metallurgical Research Laboratory and Hyderabad, India for his continued encouragement and permission to publish this work.

References

[1] Garner FA, Brager HR, Gelles DS, Mc JM. Carthy J Nucl Mater 1987;148:294–301.
[2] Hosoi Y, Okazaki Y, Wade N, Mytyabara K. J Nucl Mater 1989;169:257–62.
[3] Sarvanan Pandurangan, Raja VS. J Steel Relate Mater 2011;9:194–8.
[4] du Tolt Madeleine. J Mater Eng Perf 2002;11:306–12.
[5] Raj Baldev, Shankar P, Jayakumar T. Advances in stainless steel. 2010. p. 342.
[6] Kotecki DJ, Sievert TA. Weld J 1992:171–8.
[7] Hazra Mrityunjoy, Rao Kotipalli Srinivasa, Reddy Gankidi Madhusudhan. J Mat Res Technol 2014;1:90–100.
[8] Talha Mohd, Behera CK, Sinha OP. J materials Science Eng C 2013;7:3563–75.
[9] Parvathavarthini N, Dayal RK, Seshadri SK, Gnanamoorthy JB. J Nucl Mater 1989;2:83–8.
[10] Fu Yao, Wu Xinqiang, Han En-hou, Ke Wei, Yang Ke, Jiang Zhouhua. J. Electrochemical Acta 2009:1618–29.